

## Imaging of radiocarbon-labelled tracer molecules in neural tissue using accelerator mass spectrometry

R. E. M. Hedges\*, Z. X. Jiang\*, C. Bronk Ramsey\*,  
A. Cowey†, J. D. B. Roberts‡ & P. Somogyi‡

\* Radiocarbon Accelerator Unit, Research Laboratory for Archaeology,  
6 Keble Road, Oxford OX1 3QJ, UK

† Department of Experimental Psychology, South Parks Road,  
Oxford OX1 3UD, UK

‡ MRC Anatomical Neuropharmacology Unit, Department of Pharmacology,  
Mansfield Road, Oxford OX1 3TH, UK

AUTORADIOGRAPHY is widely and successfully used to image the distribution of radiolabelled tracer molecules in biological samples. The method is, however, limited in resolution and sensitivity, especially for  $^{14}\text{C}$ . Here we describe a new method for imaging  $^{14}\text{C}$ -labelled tracers in sections of biological tissue. A highly focused beam of gallium ions bombards the tissue, which is eroded (sputtered) into constituent atoms, molecules and secondary ions. The  $^{14}\text{C}$  ions are detected in the secondary beam by the most sensitive method available, namely accelerator mass spectrometry<sup>1</sup>. The specimen is scanned pixel by pixel ( $1 \times 2 \mu\text{m}$ ), generating an image in a manner analogous to scanning electron microscopy. The method can thus be regarded as a specialized form of scanning secondary ion mass spectrometry (SIMS), referred to here as SIAMS (ref. 2). We have used SIAMS to localize the neurotransmitter  $\gamma$ -aminobutyric acid (GABA) in thin sections of cerebral cortex, and show that it can generate  $^{14}\text{C}$  images that are much improved on  $^{14}\text{C}$  autoradiography. A scan takes 10–20 min and reveals individual axons, neurons and glial cells at high sensitivity. In principle, the resolution could be increased by up to tenfold, and the method could be extended to some other nuclides.

The essential arrangement is shown in Fig. 1. Specimens for the current application were in the form of 0.1–0.5- $\mu\text{m}$ -thick sections

cut from epoxy-embedded tissue, which were scanned by a 24 KeV Ga<sup>+</sup> beam of 1 nA, with a spot size of ~1 μm diameter. The scanning area is divided into 100 × 100 pixels, with a dwell time of 30 ms per pixel, so a complete scan takes about 5 min and sputters ~10% of the material in the field of view. A negatively charged secondary beam resulting from the sputter bombardment is extracted and injected without further mass analysis into the accelerator mass spectrometry (AMS) system. <sup>14</sup>C ions in the beam are individually detected with an efficiency of ~25% (with respect to the secondary C<sup>-</sup> beam). The AMS system has been optimized for detection of <sup>14</sup>C from archaeological samples (<sup>14</sup>C/<sup>12</sup>C ~ 10<sup>-12</sup>–10<sup>-15</sup>), for which it is normally dedicated<sup>3</sup>. In this application<sup>2,4</sup>, we directly inject the secondary beam without prior selection of mass 14, which allows <sup>14</sup>C to be unambiguously detected for <sup>14</sup>C/<sup>12</sup>C > 10<sup>-11</sup>. This approach has the advantage of making the detection efficiency insensitive to changes in the specimen voltage as a result of charge build-up on the partially insulating surface of the specimen caused by the primary ion beam. A typical count rate for detected <sup>14</sup>C is 50 Hz for a <sup>14</sup>C/<sup>12</sup>C ratio of 10<sup>-6</sup>. The same system permits imaging in <sup>13</sup>C or in <sup>12</sup>C, in which case the field is imaged simultaneously, whereas imaging in real time (TV frame rates) is possible using the total negative ion beam. In principle, other ion beams may be used for imaging (such as <sup>12</sup>C<sup>15</sup>N<sup>-</sup>), but we have not explored these possibilities.

The critical parameters for performance are the spatial resolution of the primary beam, and the <sup>14</sup>C signal obtained from a minimal level of radiocarbon label. The primary beam is provided by a VG MIG102 gun, with a limiting resolution of 0.2 μm diameter; ion extraction optics and mechanical design limit present operation to ~1 μm, but submicrometre resolution is feasible. Note, however, that the minimum adequate <sup>14</sup>C concentration is inversely proportional to voxel size and hence to the cube of the beam diameter. The minimum adequate <sup>14</sup>C concentration at 1 μm is determined by the ratio of C<sup>-</sup> ions generated by sputtering to carbon atoms sputtered. This depends on ion source operational conditions, but a ratio of ~0.01 can be reliably achieved. Thus, taking into account the 25% detection efficiency, for every 400 <sup>14</sup>C atoms sputtered, one is detected. It is necessary to pretreat the sample with evaporated caesium, decreasing its work function, in order to achieve this. In practice, the minimum adequate <sup>14</sup>C concentration depends on the <sup>14</sup>C contrast and scale of the material being imaged, but we generate images with ~20 counts per pixel from locally averaged values of <sup>14</sup>C/<sup>12</sup>C ~ 10<sup>-6</sup>, with the resolution demonstrated here. The AMS system is designed to measure isotope ratios with minimal systematic error while isotopic discrimination during sputtering from epoxy-impregnated tissue is quite constant. This method therefore enables the <sup>14</sup>C-label concentration (relative to bulk carbon) to be quantified with negligible systematic error. (To quantify the

absolute abundance, account must be taken of the local epoxy concentration and the tissue carbon content.) Our specialized form of scanning secondary ion mass spectrometry (SIAMS) could be applied to other nuclides, provided they can be detected with comparably high efficiency. Candidate nuclides include <sup>3</sup>H and <sup>36</sup>Cl, and provided label concentrations can be sufficiently increased over natural background abundance, <sup>17</sup>O, <sup>36</sup>S and <sup>15</sup>N could also be usefully imaged by SIAMS.

The cerebral cortex in the rat brain was chosen to test the potential of the method, because it is a very heterogeneous system consisting of many functionally and neurochemically distinct cellular elements, and requires high-resolution methods to dissect its components. We introduced into the brain a <sup>14</sup>C-labelled amino-acid neurotransmitter, GABA (4-amino-*n*-[U-<sup>14</sup>C]butyric acid), which is selectively taken up by those neurons that normally release it as their transmitter and so also have selective GABA re-uptake and transport mechanisms<sup>5,6</sup>, exploited previously in the neurochemical characterization of cells by autoradiography<sup>7</sup>. Glial cells also take up GABA<sup>8</sup>, contributing to the elimination of neurotransmitter from the extracellular space. The brain tissue was fixed with a mixture of aldehydes that covalently bound the accumulated transmitter to proteins and thus prevented its loss during tissue processing. The use of thin sections (50–500 nm; prepared by epoxy embedding) enabled individual cells to be characterized at high resolution by immunohistochemistry and electron microscopy, as well as by previously developed criteria for cellular categorization. The experimental design allowed the neurochemical characterization of single neurons and glial cells as well as single axons of 0.3–0.6 μm diameter in the cerebral cortex.

Figure 2 shows serial sections of the rat cortex imaged for <sup>14</sup>C for the distribution of GABA, using antibodies or toluidine-blue stain. The SIAMS images have a pixel size of 2 × 1 μm, somewhat larger than the primary beam. The (linear) <sup>14</sup>C/<sup>12</sup>C ratio in each pixel is colour coded (from blue to red). Where no <sup>14</sup>C is detected, the <sup>12</sup>C intensity image enables epoxy-plus-tissue areas to be distinguished from epoxy-only areas at low contrast, and epoxy-filled <sup>14</sup>C-deficient blood vessels can be recognized and used as landmarks. SIAMS imaging reveals the presence of high concentrations of [<sup>14</sup>C]GABA in small scattered patches that in consecutive toluidine-blue-stained sections could be identified as neurons (Fig. 2c) or, close to the injection sites, also as glial cells (Fig. 3). Smaller labelled patches revealed in SIAMS were difficult to identify in the toluidine-blue-stained sections used for light microscopy. But as up to two scans of the quality of Fig. 2 were also achieved on sections of ~100 nm thick, we used transmission electron microscopy on sections consecutive to those scanned in SIAMS to determine whether small profiles were glial cells (Fig. 3), groups of [<sup>14</sup>C]GABA-containing nerve term-

FIG. 1 The SIAMS system. Secondary ions generated from the sample on the stage (left) are injected (zero field in injection magnet) into the 2 MV tandem accelerator, and <sup>14</sup>C<sup>3+</sup> is detected after mass spectrometry at the analyser magnet and velocity filter. Other ion beams are measured at beam waists F1, F3, F12, F13, by Faraday cups or by particle detectors, as appropriate.

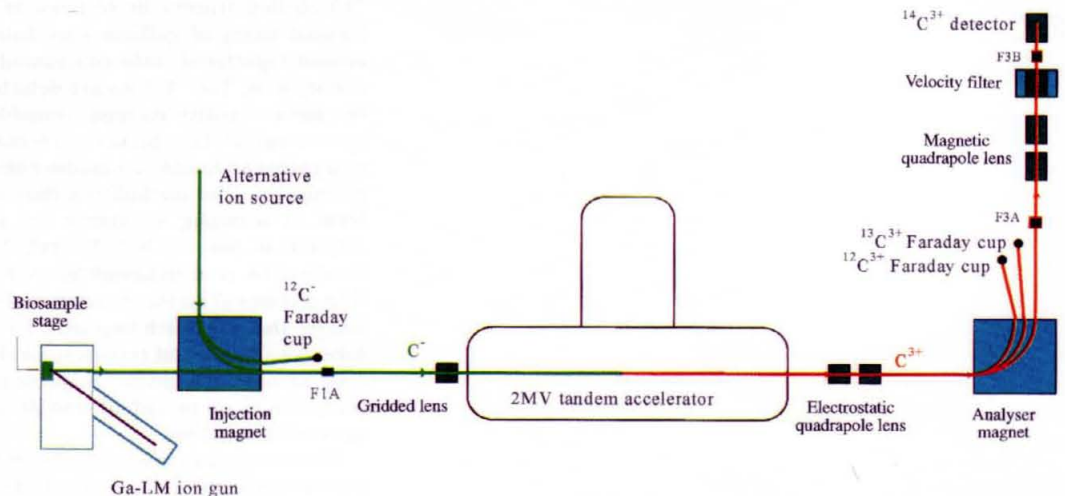
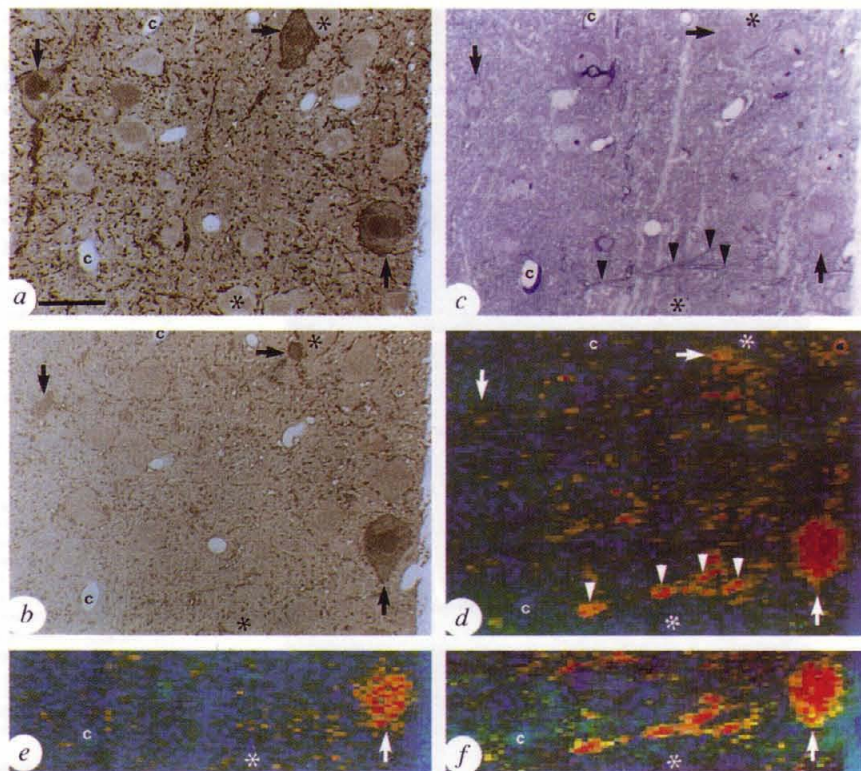


FIG. 2 Identification of [ $^{14}\text{C}$ ]GABA-accumulating neurons in layer 4 of the visual cortex of rat using SIAMS. Serial sections (0.5  $\mu\text{m}$  thick) of the same cells were immunoreacted to reveal GABA using antibodies (a and b, sections 1 and 8 respectively), stained with toluidine blue (c, section 5) or bombarded with a scanning gallium beam of  $\sim 1\ \mu\text{m}$  in diameter, followed by AMS to detect the distribution of  $^{14}\text{C}$  (d–f). The images on d and e were obtained from section 6 in the series in two separate scans taken several weeks apart. The image in f was obtained from section 3, and all three images are displayed as a ratio of  $^{14}\text{C}/^{12}\text{C}$  in each pixel (red highest, blue lowest). There are three GABA-immunopositive neuronal cell bodies (arrows) in this field, one of which (vertical arrow on right) is apparent in all 5 sections and is heavily labelled by [ $^{14}\text{C}$ ]GABA, demonstrating that it selectively accumulates this neurotransmitter. The sectioned area of the cell body of the two other GABAergic neurons diminishes as the series progresses (b), but the uppermost neuron (horizontal arrow) can be identified as labelled even when small. The neuron to the left (vertical arrow) is clearly present in the toluidine-blue-stained section (c), but appears unlabelled in the next section (d). Most other neurons (for example, asterisks) are immunonegative for GABA, but they are surrounded by small brown GABA-immunopositive puncta corresponding to nerve terminals and axons, which are also scattered throughout the neuropil. The presence of  $^{14}\text{C}$  in axons and terminals of the neuropil inevitably gives rise to scattered labelling in the SIAMS images as compared to the empty resin at the edge of the material (blue strip, right). The GABA immunonegative neurons (asterisks) and the lumen of capillaries (c) appear as cold islands in the SIAMS images. Some large myelinated axons (arrowheads) of 0.3–0.6  $\mu\text{m}$  diameter (identified in c) are very heavily labelled (d, e). Because only the cytoplasm and not the myelin sheath of the axon contains GABA, and the immunoreacted sections in a and b are several micrometres from the



edge of the material (blue strip, right). The GABA immunonegative neurons (asterisks) and the lumen of capillaries (c) appear as cold islands in the SIAMS images. Some large myelinated axons (arrowheads) of 0.3–0.6  $\mu\text{m}$  diameter (identified in c) are very heavily labelled (d, e). Because only the cytoplasm and not the myelin sheath of the axon contains GABA, and the immunoreacted sections in a and b are several micrometres from the

SIAMS images, it is not possible to identify the location of the axons in a and b. The SIAMS image of the axons appears larger than that in c, because the pixel size ( $2 \times 1\ \mu\text{m}$ ) falsely spreads the label from its real, more restricted site. The area is about 350  $\mu\text{m}$  lateral to the site of [ $^{14}\text{C}$ ]GABA injection. Scale bar, 20  $\mu\text{m}$ .

inals, or small profiles of neuronal cell bodies. For example, in the area shown in Fig. 3, it was difficult to decide which patches of high  $^{14}\text{C}$  content corresponded to neurons or glial cells. Electron microscopic examination revealed that two of the patches represented adjoining astroglial cells in direct membrane apposition and giving a labelled area similar in size to that of neurons. Glial cells were identified on the basis of the small smooth outlined nucleus, the thin rim of cytoplasm and the lack of synaptic junctions on their surface as established from serial sections. In contrast, both labelled and unlabelled neurons received numerous synaptic junctions on their soma. In a pattern identical to a previous autoradiographic demonstration of GABA uptake in cortex<sup>9,10</sup> only a small proportion of neurons were labelled even in the vicinity of the injection tracks. Using antibodies specifically recognizing fixative-modified GABA, it was found that the neurons containing  $^{14}\text{C}$  were also immunopositive for GABA. Immunostaining was not solely the result of the injection of radiolabelled GABA, however, because the frequency of immunolabelled neurons was the same in the injected area as in uninjected parts of the cortex, immunostaining of  $^{14}\text{C}$ -containing neurons was only rarely enhanced. It appears that the injected transmitter either does not significantly increase GABA levels and/or in the  $\sim 0.5$ –1 h from the injection to fixation of GABA, the radiolabelled pool replaces some of the endogenous pool. In addition, not all neurons that were immunostained for GABA were found to concentrate  $^{14}\text{C}$  (Fig. 2), which is to be expected if the uptake of transmitter occurs through the nerve terminals and GABA is then transported retrogradely to the cell body through the axon. Consequently, neurons only accumulate exogenously applied GABA if a large proportion of their terminals are close to the injection site. Different types of GABAergic neurons have

axonal arborizations oriented differentially in a characteristically inter- and intralaminar manner in the cortex<sup>9–14</sup>. In addition to cell bodies, in several cases  $^{14}\text{C}$ -rich hot-spots could be correlated with individual myelinated axons of 0.3–0.6- $\mu\text{m}$  inner thickness, demonstrating the high-resolution potential of the method. These myelinated axons belong to the largest GABAergic cells with the widest axonal arborizations<sup>12</sup>, such as one of the cells shown in Fig. 2 (upward-pointing arrow).

We have shown how uptake of labelled GABA by GABAergic neurons can be demonstrated using a new microscopic method. A measurement can be made within 24 hours of sample preparation, takes about 30 min, and is generally applicable to thin sections of epoxy-impregnated tissues. The resolution is limited by that of the primary ion beam (about 1  $\mu\text{m}$  in this work) and the label concentration, but 0.2–0.1  $\mu\text{m}$ , which we did not attempt here, appears feasible. The label concentration required for the present instrument is in the region of  $^{14}\text{C}/^{12}\text{C} = 10^{-7}$  at 1  $\mu\text{m}$  and  $^{14}\text{C}/^{12}\text{C} = 10^{-4}$  at 0.1  $\mu\text{m}$ . Although the resolution in the current example is comparable to that of using  $^3\text{H}$ -labelled molecules for autoradiography<sup>15</sup>, such as long exposure time, the limited detection of weak  $\beta$ -radiation from the depth of the sections, and the many complex issues of quantifying the absolute levels of labelled molecules are avoided by SIAMS.

We believe this novel and fast method of atomic analysis of complex heterogeneous systems such as the cerebral cortex has great potential for dissecting molecular composition and interactions, and can be combined for multiple labelling with many other methods such as immunocytochemistry. A further promising application is the quantitative high-resolution cellular mapping of metabolic activity in the brain that takes advantage of the widely

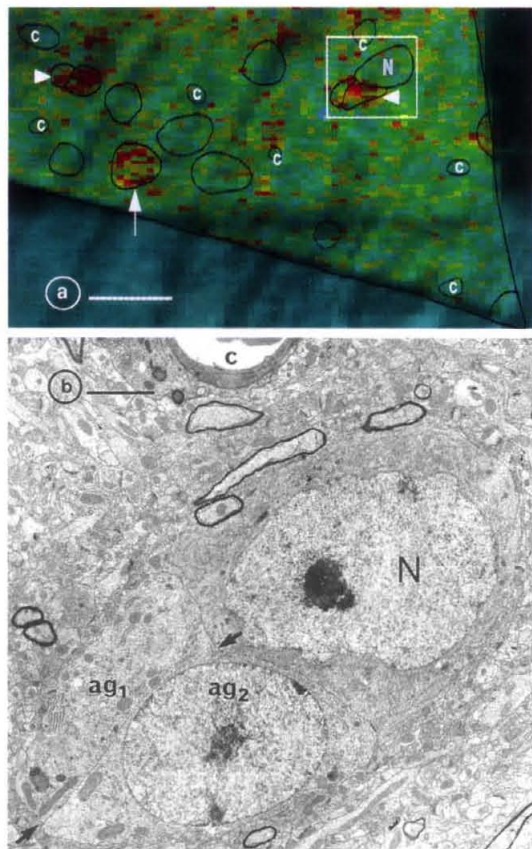


FIG. 3 Identification of [ $^{14}\text{C}$ ]GABA-accumulating cells in layer 4 of the visual cortex of rats using SIAMS (a) correlated with transmission electron microscopy (b) in serial sections (a, 100 nm thick; b, 70 nm thick). a, The corner of an ultrathin section contains three areas of high  $^{14}\text{C}$  content of about the same size. Electron microscopic examination revealed that one of them (vertical arrow) corresponds to a non-pyramidal neuron, whereas the other two represent two adjoining  $^{14}\text{C}$ -labelled glial cells each (triangles). Black lines outline the edge of the section, capillaries (c), labelled and unlabelled neurons and labelled glial cells as identified in consecutive light and electron microscopic sections. b, The framed area in a is shown in the consecutive electron microscopic section where a capillary, an unlabelled neuron (N) and the two astroglial cells ( $\text{ag}_1, \text{ag}_2$ ) can be identified. The boundary between the glial cells is indicated (arrows). Scale bars: a, 20  $\mu\text{m}$ ; b, 2  $\mu\text{m}$ .

used 2-deoxy[ $^{14}\text{C}$ ]glucose technique<sup>16</sup>. SIAMS is applicable to electron microscopic sections of about 80–100 nm thick, which further increases the resolution of the localization as well as the identification of the cellular components. It will be important to increase both the resolution and the sensitivity further for the quantitative localization of ligand binding sites by neurotransmitter receptors and ion channels which can only be localized at present with low resolution. The prospect of using ligands labelled with different isotopes shows how SIAMS imaging can potentially reveal the molecular machinery of chemical communication in the brain. □

## Methods

Two adult Wistar rats were deeply anaesthetized with sodium pentobarbital (Sagatal; 45 mg kg<sup>-1</sup>, i.p., supplemented as required) and mounted in a stereotaxic apparatus. Following a small craniotomy, the occipital cortex was injected unilaterally through glass micropipettes (tip, 30–50  $\mu\text{m}$ ) at two sites, perpendicular to the superior sagittal sinus and at 40 degrees to the vertical plane. Radiolabelled GABA (209 mCi mmol<sup>-1</sup>, Amersham) was dissolved in artificial cerebrospinal fluid at a concentration of 0.95 mM, diluted further by the injection into the brain. Along each track (4–5 mm tangentially, latero-ventral from the pia), 5–8 injections were placed 0.5 mm apart delivering a total of 0.75  $\mu\text{l}$  GABA

(~700 nmol), slowly over 15 min. Animals received an overdose of anaesthetic 50 min after the start of the first injection, followed by transcardial perfusion with a fixative containing 2.5% glutaraldehyde, 0.5% paraformaldehyde in 0.1 M phosphate buffer. The brains were sectioned sagittally (cross sectioning to the tracks), the sections (60- $\mu\text{m}$ -thick) were treated with osmium tetroxide (0.1%) to reduce shrinkage, and embedded in epoxy resin (Durcupan, Fluka)<sup>10,11</sup>. Strips of cortex (0.2–0.3 mm wide) from pia to white matter at different lateral distances from the injection tracks were sectioned further at 0.5  $\mu\text{m}$  thickness on an ultramicrotome. Serial sections were alternately mounted either on Al stubs for SIAMS, or on glass slides for either the immunocytochemical visualization of GABA<sup>17</sup> using polyclonal antibodies (diluted 1:6,000)<sup>18</sup> and the indirect immunoperoxidase method, or for toluidine-blue-staining to reveal cellular elements in the light microscope. The sections for electron microscopy were picked up on pioloform-coated single-slot grids, and contrasted with uranyl acetate and lead citrate.

Received 1 April; accepted 5 September 1996.

1. Litherland, A. E. *Phil. Trans. R. Soc. Lond. A* **323**, 5–21 (1987).
2. Freeman, S. P. H. T., Bronk Ramsey, C. & Hedges, R. E. M. *Nucl. Instr. Meth. B* **93**, 231–236 (1993).
3. Hedges, R. E. M. *Phil. Trans. R. Soc. Lond. A* **323**, 57–72 (1987).
4. Jiang, Z. X., Bronk Ramsey, C. & Hedges, R. E. M. *Nucl. Instr. Meth. B* (in the press).
5. Martin, D. L. in *GABA in Nervous System Function* (eds Roberts, E., Chase, T. N. & Tower, D. B.) 347–386 (Raven, New York, 1976).
6. Hokfelt, T. & Ljungdahl, A. *Exp. Brain Res.* **14**, 354–362 (1972).
7. Cuenod, M. & Streit, P. in *Methods in Chemical Neuroanatomy* (eds Bjorklund, A. & Hokfelt, T.) 365–397 (Elsevier, Amsterdam, 1983).
8. Hertz, L. *Prog. Neurobiol.* **13**, 277–323 (1979).
9. Somogyi, P., Cowey, A., Halasz, N. & Freund, T. F. *Nature* **294**, 761–763 (1981).
10. Somogyi, P., Kisvarday, Z. F., Freund, T. F. & Cowey, A. *Exp. Brain Res.* **53**, 295–303 (1984).
11. Somogyi, P., Freund, T. F. & Kisvarday, Z. F. *Exp. Brain Res.* **54**, 45–56 (1984).
12. Somogyi, P., Cowey, A., Kisvarday, Z. F., Freund, T. F. & Szentagothai, J. *Proc. Natl Acad. Sci. USA* **80**, 2385–2389 (1983).
13. Somogyi, P., Kisvarday, Z. F., Martin, K. A. C. & Whitteridge, D. *Neuroscience* **10**, 261–294 (1983).
14. Kisvarday, Z. F., Martin, K. A. C., Friedlander, M. J. & Somogyi, P. *J. Comp. Neurol.* **260**, 1–19 (1987).
15. Baker, J. R. J. *Autoradiography: A Comprehensive Overview* (Microscopy Handbooks, Vol. 18) (Oxford University Press, Oxford, 1989).
16. Duncan, G. E. & Stumpf, W. E. in *Quantitative and Qualitative Microscopy; Methods in Neurosciences* Vol. 3 (ed. Conn, P. M.) 50–64 (Academic, New York, 1990).
17. Somogyi, P., Hodgson, A. J., Chubb, I. W., Penke, B. & Erdi, A. *J. Histochem. Cytochem.* **33**, 240–248 (1985).
18. Hodgson, A. J., Penke, B., Erdi, A., Chubb, I. W. & Somogyi, P. *J. Histochem. Cytochem.* **33**, 229–239 (1985).

ACKNOWLEDGEMENTS. We thank the MRC Brain and Behaviour Centre for financial support. We acknowledge valuable discussion with S.P.H.T. Freeman and the contribution of Z. Nusser at the initial stages of test sample preparations.

CORRESPONDENCE and requests for materials should be addressed to R.E.M.H., A.C. or P.S.

Nature, 20 November 1997, Vol. 390, No. 6657, page 315

## Imaging of radiocarbon-labelled tracer molecules in neural tissue using accelerator mass spectrometry

R. E. M. Hedges, Z. X. Jiang, C. Bronk Ramsey, A. Cowey, J. D. B. Roberts & P. Somogyi

*Nature* **383**, 823–826 (1996)

We regret that we did not refer in this Letter to two publications<sup>1,2</sup>. These authors showed that scanning SIMS (rather than SIAMS) can be used in a similar way to image tracers, including  $^{14}\text{C}$ , in tissue. We had not appreciated, from the published data, the extent to which the performance of the instrument might be equivalent to that of SIAMS. □

1. Slodzian, G., Diagne, B., Girard, F., Boust, F. & Hillion, F. Scanning secondary ion analytical microscopy with parallel detection. *Biology of the Cell* **74**, 43–50 (1992).
2. Hindié, E., Coulomb, B., Beaupin, R. & Galle, P. Mapping the cellular distribution of labelled molecules by SIMS microscopy. *Biology of the Cell* **74**, 82–88 (1992).